

## LOW-COMPLEXITY GAIN AND PHASE I/Q MISMATCH COMPENSATION USING ORTHOGONAL PILOT SEQUENCES

Luca Giugno<sup>1</sup>, Vincenzo Lottici<sup>2</sup> and Marco Luise<sup>2</sup>

<sup>1</sup>Wiser S.r.l. – Wireless Systems Engineering and Research  
Via Fiume 23, 57123, Livorno, Italy  
phone: + (39) 0586 888487, fax: + (39) 0586 888487, email: [luca.giugno@wiser.it](mailto:luca.giugno@wiser.it)

<sup>2</sup>University of Pisa – Dipartimento di Ingegneria dell'Informazione  
Via G. Caruso, 56122, Pisa, Italy  
phone: + (39) 050 2217511, fax: + (39) 050 2217522, email: [{m.luise;v.lottici}@iet.unipi.it](mailto:{m.luise;v.lottici}@iet.unipi.it)

### ABSTRACT

*In up-to-date receiver architectures the gain and phase mismatch between the I and Q signal paths may degrade significantly the overall link performance. An alternative cost effective solution to expensive analog components with small tolerances, which make the I/Q mismatch effect negligible, consists in estimating and compensating it through appropriate digital signal processing techniques. In this paper we derive a novel low-complexity data-aided scheme for jointly estimating the carrier phase offset, the I/Q phase mismatch, and the gain of the I and Q branches following the maximum likelihood criterion and adopting as training symbols an orthogonal sequence. The performance analysis proves that the proposed estimator is low-complexity, asymptotically efficient and capable of compensating considerable I/Q mismatch values in the demanding scenario of both uncoded and coded multi-level QAM transmissions.*

### 1. INTRODUCTION

The currently widespread applications of radio frequency (RF) transceivers have motivated the study and development of innovative architectures for frequency conversion. Several significant schemes have been proposed as alternative solutions to the conventional heterodyne architecture that has been utilized so far in most of commercially available RF devices for its good selectivity and sensitivity performance, but does come with the inherent drawback of requiring a relatively large form factor due to the non-integrable RF and IF filters. We recall the direct conversion mixers [1]-[2], wherein the RF signal is demodulated directly to baseband, and the low-IF architecture [3]. All the aforementioned schemes, however, make use of quadrature mixing which in turn, due to the finite tolerances of the components in the analog section, actually exhibits both errors in the nominally 90° phase shift and gain mismatches between the in-phase (I) and quadrature (Q) signal paths, a fact that contributes to corrupt the demodulated signal and increase inevitably performance degradation. Indeed, just adopting a cautious yet expensive analog design, only gain and phase mismatch of 1° ÷ 2° and 1% ÷ 2%, respectively, are realistically achievable [1]. This means that in a typical up-to-date low-cost and

low-complexity transmitter/receiver scheme considerable degradation of the overall communication link performance is avoided only on condition that the I/Q mismatch effect is adequately compensated for. Large emphasis has been addressed recently to the issue of gain and phase I/Q mismatch estimation and cancellation in quadrature processing receivers, as shown by [4]-[10]. Simple methods consist in estimating off-line at the receiver the mismatch parameters by means of a calibration test-tone [4], or employing a Gram-Schmidt orthogonalization procedure [5]. An alternative scheme for low-IF receivers is introduced in [6]. The technique proposed in [7], instead, jointly estimates the I/Q mismatch and the DC-offset values along with the overall channel impulse response in a least-square (LS) sense employing a properly designed training sequence. In addition, the interesting extension of [7] is pursued in [8] following a data-aided maximum likelihood (ML) approach, with particular emphasis on the frequency offset and channel estimation issues. To end with this survey on I/Q mismatch estimation, we call to mind quite different adaptive schemes, such as the data-aided (DA) procedure introduced in [9] and that based on interference cancellation (IC) or blind source separation (BSS) algorithms proposed in [10]. The above estimators lead to significant performance improvement, nevertheless come with the inherent drawback of requiring a “learning” interval during which the filter adaptation has to be done according to least mean square (LMS) or recursive least squares (RLS) rules. Consequently, they should turn out to be impractical for short packet wireless. In this paper, we pursue a further different approach proposing a DA joint estimator of the carrier phase offset, the I/Q phase mismatch, and the gain of the I and Q signal paths, suited to be applied in the case of low-IF receivers for which the DC-offset does not represent a serious concern. Following the ML optimality criterion and through judicious choice of training data symbols based on orthogonal sequence, we end up to a low-complexity and asymptotically efficient estimation scheme capable of compensating considerable I/Q mismatch values in the demanding scenario of both uncoded and coded multi-level QAM transmissions. The motivation of the study stems mainly from the needs arising from the application of typical low-cost end-user consumer receivers in the high-rate satel-

lite broadcasting context, wherein reasonably the following operating conditions are expected to hold: i) since direct-conversion receiver architectures are typically avoided, the DC-offset can be easily suppressed in most situations; ii) the transmission channel is usually non-frequency selective, and accordingly, has not to be estimated; iii) carrier frequency and timing synchronization is assumed to be recovered for instance through the methods outlined in [11].

## 2. SYSTEM MODELING

Let us focus on the block diagram of Fig. 1 representing the receiver of a typical wireless communications link, and assume that the received signal can be written as

$$r_{RF}(t) = I(t)\cos 2\pi f_0 t - Q(t)\sin 2\pi f_0 t + n_{RF}(t) \quad (1)$$

where  $f_0$  is the carrier frequency,  $n_{RF}(t)$  is a white Gaussian noise process with (two-sided) power spectral density equal to  $N_0/2$ , whereas  $I(t)$  and  $Q(t)$  denote the I and Q components of the useful signal given by

$$I(t) = \sum_i a_i g(t - iT) \quad (2)$$

$$Q(t) = \sum_i b_i g(t - iT) \quad (3)$$

In (2)-(3), the symbols  $a_i$  and  $b_i$  belong to the M-QAM alphabet  $S = \{\pm 1, \pm 3, \dots, \pm\sqrt{M} - 1\}$ ,  $g(t)$  is a square root raised cosine (SRRC) shape with roll-off factor  $\eta$  and  $T$  represents the signaling interval. Let us now indicate with  $\vartheta$  the carrier phase offset between the received signal and the local reference, with  $\rho \triangleq B/A$  and  $\varphi$  the I/Q amplitude and phase mismatch, respectively, with  $A$  and  $B$  being the gains of the in-phase and quadrature signal paths. Frequency conversion of  $r_{RF}(t)$  in (1) and low-pass filtering through  $h_{LP}(t)$  yield [10]

$$u(t) = A \cdot I(t)\cos(2\pi f_d t + \vartheta) + A \cdot Q(t)\sin(2\pi f_d t + \vartheta) \quad (4)$$

$$v(t) = B \cdot I(t)\sin(2\pi f_d t + \vartheta + \varphi) + B \cdot Q(t)\cos(2\pi f_d t + \vartheta + \varphi) \quad (5)$$

where  $f_d \triangleq f_{LO} - f_0$  is the residual carrier frequency offset,  $f_{LO}$  being the local receiver reference. Notice here that  $f_d$  can be estimated employing the well-known DA carrier recovery schemes proposed in the literature so far, as found for instance in [12]. Hence, for the sake of simplicity we will adopt henceforth ideal carrier frequency recovery condition, i.e.,  $f_d = 0$ . Assuming ideal timing recovery as well, the output of the receiver matched filter can be expressed as

$$x(k) \triangleq x_I(k) + jx_Q(k) = A[a_k \cos \vartheta + b_k \sin \vartheta] + jB[b_k \cos(\vartheta + \varphi) - a_k \sin(\vartheta + \varphi)] + w(k) \quad (6)$$

where  $w(k) \triangleq w_I(k) + jw_Q(k)$  is the complex-valued AWGN component,  $w_I(k)$  and  $w_Q(k)$  being independent zero-mean white Gaussian discrete-time process each with variance equal to  $\sigma^2$ . Defining

$$\Psi(\vartheta, \varphi, A, B) \triangleq \begin{bmatrix} A \cos \vartheta & A \sin \vartheta \\ -B \sin(\vartheta + \varphi) & B \cos(\vartheta + \varphi) \end{bmatrix} \quad (7)$$

and employing the real and imaginary components of both  $x(k)$  and  $w(k)$  make re-arrange (5) as [10]

$$\begin{bmatrix} x_I(k) \\ x_Q(k) \end{bmatrix} = \Psi(\vartheta, \varphi, A, B) \begin{bmatrix} a_k \\ b_k \end{bmatrix} + \begin{bmatrix} w_I(k) \\ w_Q(k) \end{bmatrix} \quad (8)$$

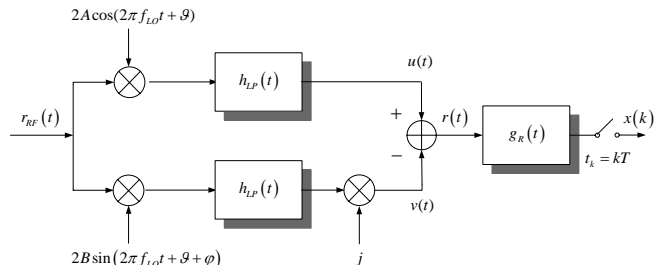


Fig. 1 – I/Q demodulator with I/Q amplitude and phase mismatch.

The above equation suggests a low-complexity way to get rid of the effect of I/Q amplitude and phase mismatch. Indeed, let us assume that reliable estimates, say  $\hat{\vartheta}$ ,  $\hat{\varphi}$ ,  $\hat{A}$  and  $\hat{B}$ , of  $\vartheta$ ,  $\varphi$ ,  $A$  and  $B$ , respectively, are available by properly processing the preamble containing a known pilot sequence, according to what we will propose in the next section. Thus, applying

$$\begin{bmatrix} y_I(k) \\ y_Q(k) \end{bmatrix} = \Psi^{-1}(\hat{\vartheta}, \hat{\varphi}, \hat{A}, \hat{B}) \begin{bmatrix} x_I(k) \\ x_Q(k) \end{bmatrix} \quad (9)$$

with

$$\Psi^{-1}(\hat{\vartheta}, \hat{\varphi}, \hat{A}, \hat{B}) = \frac{1}{\hat{A}\hat{B}\cos\hat{\varphi}} \begin{bmatrix} \hat{B}\cos(\hat{\vartheta} + \hat{\varphi}) & -\hat{A}\sin\hat{\vartheta} \\ \hat{B}\sin(\hat{\vartheta} + \hat{\varphi}) & \hat{A}\cos\hat{\vartheta} \end{bmatrix} \quad (10)$$

enables to compensate prior to the decoding step the receiver matched filter samples within the payload section.

## 3. JOINT CARRIER PHASE OFFSET, I/Q PHASE MISMATCH, AMPLITUDE AND I/Q AMPLITUDE MISMATCH ESTIMATION

This section deals with the derivation of the joint DA maximum-likelihood (ML) estimator for the abovementioned parameters  $\vartheta$ ,  $\varphi$ ,  $A$  and  $B$ . Stacking in the vector  $\mathbf{x} \triangleq [x(0), x(1), \dots, x(N-1)]^T$  the samples at the output of the receiver matched filter corresponding to the preamble of  $N$  known complex-valued data symbols  $c_k \triangleq a_k + jb_k$ , the likelihood function (LF) for the unknown parameters  $\vartheta$ ,  $\varphi$ ,  $A$  and  $B$  (up to irrelevant multiplicative factors) can be written as

$$\Lambda(\mathbf{x} | \tilde{\vartheta}, \tilde{\varphi}, \tilde{A}, \tilde{B}) = e^{-\frac{1}{\sigma^2} \operatorname{Re} \left\{ \sum_{k=0}^{N-1} x(k) \tilde{s}^*(k) \right\} - \frac{1}{2\sigma^2} \sum_{k=0}^{N-1} |\tilde{s}(k)|^2} \quad (11)$$

where

$$\tilde{s}(k) \triangleq \tilde{A} [a_k \cos \tilde{\vartheta} + b_k \sin \tilde{\vartheta}] + j\tilde{B} [b_k \cos(\tilde{\vartheta} + \tilde{\varphi}) - a_k \sin(\tilde{\vartheta} + \tilde{\varphi})] \quad (12)$$

is the trial signal replica with  $\tilde{\vartheta}$ ,  $\tilde{\varphi}$ ,  $\tilde{A}$  and  $\tilde{B}$  trial values of the parameters to be estimated, namely the carrier phase offset, the I/Q phase mismatch, and the gain of the I and Q branches, respectively. In order to reduce complexity, we will resort in the sequel to a training orthogonal sequence of 4-QAM symbols  $c_k = a_k + jb_k$ , with  $a_k = \pm 1$ ,  $b_k = \pm 1$  and

$$\sum_{k=0}^{N-1} a_k b_k = 0 \quad (13)$$

Hence, after dropping irrelevant factors independent of the parameters to be estimated, we are left with the log-likelihood function (LLF)

$$\Gamma(\mathbf{x}|\tilde{\vartheta}, \tilde{\varphi}, \tilde{A}, \tilde{B}) = \log(\Lambda(\mathbf{x}|\tilde{\vartheta}, \tilde{\varphi}, \tilde{A}, \tilde{B})) \quad (14)$$

that through the definitions

$$\alpha \triangleq \operatorname{Re} \left\{ \sum_{k=0}^{N-1} x(k) a_k \right\} \quad (15)$$

$$\beta \triangleq \operatorname{Re} \left\{ \sum_{k=0}^{N-1} x(k) b_k \right\} \quad (16)$$

$$\gamma \triangleq \operatorname{Im} \left\{ \sum_{k=0}^{N-1} x(k) a_k \right\} \quad (17)$$

$$\delta \triangleq \operatorname{Im} \left\{ \sum_{k=0}^{N-1} x(k) b_k \right\} \quad (18)$$

can be re-arranged as

$$\begin{aligned} \Gamma(\mathbf{x}|\tilde{\vartheta}, \tilde{\varphi}, \tilde{A}, \tilde{B}) &= \alpha \tilde{A} \cos \tilde{\vartheta} + \beta \tilde{A} \sin \tilde{\vartheta} + \\ &+ \delta \tilde{B} \cos(\tilde{\vartheta} + \tilde{\varphi}) - \gamma \tilde{B} \sin(\tilde{\vartheta} + \tilde{\varphi}) - \frac{\tilde{A}^2 N}{2} - \frac{\tilde{B}^2 N}{2} \end{aligned} \quad (19)$$

A necessary condition for a local maximum of (19) is that its derivatives with respect to  $\tilde{\vartheta}$ ,  $\tilde{\varphi}$ ,  $\tilde{A}$  and  $\tilde{B}$  are zero, that is

$$\frac{\partial \Gamma(\mathbf{x}|\tilde{\vartheta}, \tilde{\varphi}, \tilde{A}, \tilde{B})}{\partial \tilde{\vartheta}} = -\alpha \tilde{A} \sin \tilde{\vartheta} + \beta \tilde{A} \cos \tilde{\vartheta} \quad (20)$$

$$-\delta \tilde{B} \sin(\tilde{\vartheta} + \tilde{\varphi}) - \gamma \tilde{B} \cos(\tilde{\vartheta} + \tilde{\varphi}) = 0$$

$$\frac{\partial \Gamma(\mathbf{x}|\tilde{\vartheta}, \tilde{\varphi}, \tilde{A}, \tilde{B})}{\partial \tilde{\varphi}} = -\delta \tilde{B} \sin(\tilde{\vartheta} + \tilde{\varphi}) + \quad (21)$$

$$-\gamma \tilde{B} \cos(\tilde{\vartheta} + \tilde{\varphi}) = 0$$

$$\frac{\partial \Gamma(\mathbf{x}|\tilde{\vartheta}, \tilde{\varphi}, \tilde{A}, \tilde{B})}{\partial \tilde{A}} = \alpha \cos \tilde{\vartheta} + \beta \sin \tilde{\vartheta} - N \tilde{A} = 0 \quad (22)$$

$$\frac{\partial \Gamma(\mathbf{x}|\tilde{\vartheta}, \tilde{\varphi}, \tilde{A}, \tilde{B})}{\partial \tilde{B}} = \delta \cos(\tilde{\vartheta} + \tilde{\varphi}) + \quad (23)$$

$$-\gamma \sin(\tilde{\vartheta} + \tilde{\varphi}) - N \tilde{B} = 0$$

Substituting (21) into (20) gives

$$-\alpha \tilde{A} \sin \tilde{\vartheta} + \beta \tilde{A} \cos \tilde{\vartheta} = 0 \quad (24)$$

or equivalently assuming  $\tilde{A} > 0$

$$\operatorname{Re}\{(\beta + j\alpha)e^{j\tilde{\vartheta}}\} = 0 \quad (25)$$

Using (15)-(16), it follows from (25) that the estimates of the carrier phase offset is given by

$$\hat{\vartheta} = \frac{\pi}{2} - \angle(\beta + j\alpha) = \arctan \left( \frac{\operatorname{Re} \left\{ \sum_{k=0}^{N-1} x(k) b_k \right\}}{\operatorname{Re} \left\{ \sum_{k=0}^{N-1} x(k) a_k \right\}} \right) \quad (26)$$

Using the same arguments leading to (26), it is found that (21) can be rewritten as (considering  $\tilde{B} > 0$ )

$$\operatorname{Re}\{(\gamma - j\delta)e^{j(\tilde{\vartheta} + \tilde{\varphi})}\} = 0 \quad (27)$$

i.e.,

$$\hat{\vartheta} + \hat{\varphi} = \frac{\pi}{2} - \angle(\gamma - j\delta) = \arctan\left(-\frac{\gamma}{\delta}\right) \quad (28)$$

from which we get the estimate of the I/Q phase mismatch

$$\hat{\varphi} = \arctan \left( -\frac{\operatorname{Im} \left\{ \sum_{k=0}^{N-1} x(k) a_k \right\}}{\operatorname{Im} \left\{ \sum_{k=0}^{N-1} x(k) b_k \right\}} \right) - \hat{\vartheta} \quad (29)$$

It is worth noting that  $\hat{\varphi}$  given by (29) depends on  $\hat{\vartheta}$ , and estimation of the I/Q phase mismatch must be achieved only after that pertaining the carrier phase offset. As final step from (22)-(23) we obtain the estimates of the I and Q gains

$$\hat{A} = \frac{\operatorname{Re} \left\{ \sum_{k=0}^{N-1} x(k) a_k \right\} \cos \hat{\vartheta} + \operatorname{Re} \left\{ \sum_{k=0}^{N-1} x(k) b_k \right\} \sin \hat{\vartheta}}{N} \quad (30)$$

$$\hat{B} = \frac{\operatorname{Im} \left\{ \sum_{k=0}^{N-1} x(k) b_k \right\} \cos(\hat{\vartheta} + \hat{\varphi})}{N} + \quad (31)$$

$$-\frac{\operatorname{Im} \left\{ \sum_{k=0}^{N-1} x(k) a_k \right\} \sin(\hat{\vartheta} + \hat{\varphi})}{N}$$

Similarly to above, the estimate of  $A$  must be accomplished after estimation of  $\vartheta$ , whereas  $\hat{B}$  depends on  $\hat{\vartheta}$  and  $\hat{\varphi}$ .

#### 4. PERFORMANCE ANALYSIS

In this section, we verify the effectiveness of the proposed joint estimator through simulation results. First, we quantify the ultimate accuracy that can be achieved by establishing a performance limit in the form of Cramér-Rao Bound (CRB) against which we can compare the performance of our estimator. Then, the mean estimated value (MEV) and the root-mean square estimation error (RMSEE) performance metrics are calculated by simulation. Finally, we evaluate by simulations the impact of both the estimation and compensation of the carrier phase offset, the I/Q amplitude and phase mismatch, has on the BER performance of the data demodulator. In our simulations we consider the transmission of TDMA frames each composed of a preamble of  $N$  known QPSK symbols chosen as the orthogonal sequence

$$a_k = +1, \quad k = 0, \dots, N-1 \quad (32)$$

$$b_k = \begin{cases} +1, & k = 0, \dots, N/2-1 \\ -1, & k = N/2, \dots, N-1 \end{cases} \quad (33)$$

followed by a payload of  $N_b$  uncoded or turbo coded QAM information bearing data symbols. All the parameters to be estimated are considered time-invariant within the received data frame, whereas symbol timing, frame reference and carrier frequency offset are assumed to be perfectly recovered. As mentioned above, the lower limit to the RMSEE of any unbiased joint estimator is represented by the vector Cramér-Rao Bound (CRB) [13]. Due to space limitation, we did not report the derivation of the CRBs for the joint estimation of the carrier phase offset  $\vartheta$ , I/Q phase mismatch  $\varphi$ , gain  $A$  over the I branch and gain  $B$  over the Q branch, that can be expressed as

$$\text{CRB}(\vartheta) = \frac{1}{NA^2} \cdot \frac{1}{E_s/N_0} \quad (34)$$

$$\text{CRB}(\varphi) = \left[ \frac{1}{NA^2} + \frac{1}{NB^2} \right] \cdot \frac{1}{E_s/N_0} \quad (35)$$

$$\text{CRB}(A) = \frac{1}{N} \cdot \frac{1}{E_s/N_0} \quad (36)$$

$$\text{CRB}(B) = \frac{1}{N} \cdot \frac{1}{E_s/N_0} \quad (37)$$

It can be shown (not reported for space limitation) that the joint estimator is asymptotically (i.e. for large values of signal-to-noise ratio SNR) unbiased and efficient. Next, let us evaluate the MEVs of the estimators (26), (29), (30) and (31) through a simulation approach, i.e., by computing numerically the averages  $E\{\hat{\vartheta}\}$ ,  $E\{\hat{\varphi}\}$ ,  $E\{\hat{A}\}$  and  $E\{\hat{B}\}$  as a function of their respective true values  $\vartheta$ ,  $\varphi$ ,  $A$  and  $B$ , respectively, over a number of  $L=10000$  independent realizations of the parameters to be estimated. The adopted pilot sequence is given by (32)-(33) with length  $N=1000$ . The MEV curves for the carrier phase offset  $\vartheta$  shown in Fig. 2 corresponds to some values of the mean energy to noise spectral density ratio, namely  $E_s/N_0=0, 10, 20$  dB, and  $\varphi=5^\circ$ ,  $A=2$  and  $B=2.1$ , for a I/Q amplitude imbalance  $\rho=B/A=1.05$ . Instead, in Fig. 3 we depict the MEV curves for the I/Q phase mismatch  $\varphi$ , with the same values of  $A$  and  $B$  but for  $\vartheta=40^\circ$ . It is apparent that the acquisition range for the phase offset  $\vartheta$  increases with the SNR, and specifically, amounts to roughly  $\pm 170^\circ$  for the worst case of  $E_s/N_0=0$  dB, whereas the acquisition range for the I/Q phase mismatch  $\varphi$  is independent of the SNR and covers the whole range  $|\varphi| \leq 180^\circ$ . Finally, Figs. 4 and 5 depict the MEV curve for the gain  $A$  and  $B$ , respectively, with  $\vartheta=40^\circ$  and  $\varphi=5^\circ$  and the I/Q gain mismatch  $\rho$  kept fixed to 1.05. Figures 6-9 compare the RMSEE curves (marks) for the estimators (26), (29), (30) and (31), respectively, obtained through simulations choosing  $\vartheta=40^\circ$ ,  $\varphi=0^\circ$ ,  $A=2$ ,  $B=2.1$  ( $\rho=B/A=1.05$ ) and  $N=10, 100, 1000$  as preamble length, with the corresponding CRBs (solid lines) given by (34)-(37). Again, the ensemble mean operator  $E\{\cdot\}$  is approximated by its sample average over  $L=10000$

independent realizations of the parameters to be estimated. As final point, it is now of interest evaluating the impact of the proposed estimation and compensation scheme on the BER performance. Specifically, we focus on multi-level 16-QAM and 64-QAM signals that are well known to be particularly vulnerable to the I/Q amplitude and phase mismatch issue. We assume both uncoded and turbo coded transmission arranged in TDMA frames each of which encompasses a preamble of  $N=100$  known QPSK symbols to perform carrier phase offset, I/Q phase mismatch, and I and Q gain estimation, followed by a payload of  $N_b=5000$  QAM data symbols. Applying (9)-(10) to the receiver matched filter samples within the payload section enables to compensate for the I/Q mismatch and perform reliable data decoding. Concerning the turbo coded system, we adopt a PCCC (Parallel Concatenated Convolutional Code) scheme based on the parallel concatenation of two identical 16-states rate-1/2 RSC (Recursive Systematic Convolutional) encoders with generators  $g_1=(31)_8$  and  $g_2=(33)_8$  via a pseudo-random interleaver with block length  $k=15000$ . The parity bits at the output of the turbo encoder are properly punctured to obtain the desired overall rate, i.e.,  $r=3/4$  for 16-QAM and  $r=1/2$  for 64-QAM [11], [14]. In Fig. 10 we illustrate the BER performance results for uncoded 16-QAM and 64-QAM transmission as a function of the SNR in the following cases: i) ideal AWGN with no offset/mismatch; ii)  $\vartheta=40^\circ$ ,  $\varphi=5^\circ$ ,  $A=3$  and  $B=3.15$  (corresponding to the I/Q gain mismatch  $\rho=1.05$ ) with estimation/compensation of the four above parameters. Figure 11, instead, gives the BER curves of turbo-encoded  $r=3/4$  16-QAM and  $r=1/2$  64-QAM as a function of the SNR for: i) ideal AWGN with no offset/mismatch; ii)  $\vartheta=40^\circ$ ,  $\varphi=5^\circ$ ,  $A=2$  and  $B=2.1$  (corresponding to  $\rho=1.05$ ) and I/Q mismatch estimation/compensation. The simulation results confirm the effectiveness of the proposed joint estimation/compensation scheme with quite modest implementation complexity.

## 5. CONCLUSIONS

A novel low-complexity DA scheme for jointly estimating the carrier phase offset, the I/Q phase mismatch, and the gain of the I and Q branches has been derived based on the appropriate choice of orthogonal training sequence. The performance evaluated through computer simulations reveals that the proposed estimator is unbiased and asymptotically efficient offering an accuracy that achieves the corresponding CRB. BER performance evaluation of both uncoded and turbo coded multi-level QAM systems equipped with the proposed estimation/compensation method show negligible degradation in the presence of considerable I/Q mismatch values even at low SNRs.

## REFERENCES

- [1] B. Razavi, "Design Considerations for Direct-Conversion Receivers," IEEE Trans. Circuits Syst. II, vol. 44, pp. 428-435, June 1997.

- [2] A. A. Abidi, "Direct-Conversion Radio Transceivers for Digital Communications," IEEE Jour. of Solid-State Circuits, vol. 30, pp. 1399-1410, Dec. 1995.
- [3] S. Mirabbasi and K. Martin, "Classical and Modern Receiver Architecture," IEEE Commun. Mag., vol. 38, pp. 132-139, Nov. 2000.
- [4] J. P. F. Glas, "Digital I/Q Imbalance Compensation in Low-IF Receiver," IEEE Globecom 1998, Nov. 1998.
- [5] X. Huang, "On Transmitter Gain/Phase Imbalance Compensation at Receiver," IEEE Commun. Letters, vol. 4, n. 11, pp. 363-366, Nov. 2000.
- [6] C. C. Chen and C. C. Huang, "On the Architecture and Performance of a Hybrid Image Rejection Receiver," IEEE Journal on Selected Areas on Comm., vol. 19, pp. 1029-1040, June 2001.
- [7] I. H. Sohn, E. R. Jeong and Y. H. Lee, "Data-Aided Approach to I/Q Mismatch and DC Offset Compensation in Communication Receivers", IEEE Commun. Letters, vol. 6, n. 12, pp. 547-549, Dec. 2002.
- [8] G. T. Gil *et alii*, "Joint ML Estimation of Carrier Frequency, Channel, I/Q Mismatch and DC Offset in Communication Receivers," IEEE Trans. on Veh. Tech., vol. 54, n. 1, pp. 338-349, Jan. 2005.
- [9] J. K. Cavers and M. W. Liao, "Adaptive Compensation for Imbalance and Offset Losses in Direct Conversion Transceivers," IEEE Trans. on Veh. Tech., vol. 42, n. 4, p. 581-588, Nov. 1993.
- [10] M. Valkama, M. Renfors and V. Koivunen, "Advanced Methods for I/Q Imbalance Compensation in Communication Receivers," IEEE Trans. on Signal Processing, vol. 49, n. 10, pp. 2335-2344, Oct. 2001.
- [11] S. Benedetto *et alii*, "MHOMS: high-speed ACM modem for satellite applications," IEEE Pers. Commun., vol. 12, pp. 66-77, Apr. 2005.
- [12] D. C. Rife and R. R. Boorstyn, "Single Tone Parameter Estimation from Discrete-Time Observations," IEEE Trans. Inf. Theory, IT-20, pp. 591-598, Sept. 1974.
- [13] F. Gini *et alii*, "The Modified Cramér-Rao Bound in Vector Parameter Estimation," IEEE Trans. Commun., vol. 46, no.1, pp. 52-60, Jan. 1998.
- [14] C. Berrou, A. Glavieux and S. Le Goff, "Turbo-Codes and High Spectral Efficiency Modulation," IEEE ICC 1994, pp. 645-649, May 1994.

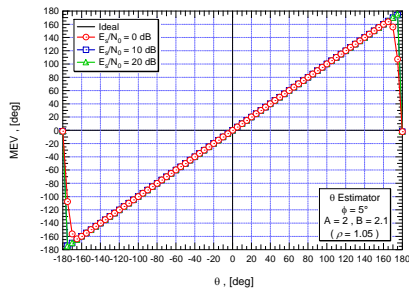


Fig. 2 – Simulated MEV of  $\theta$  for different values of  $E_s/N_0$ .

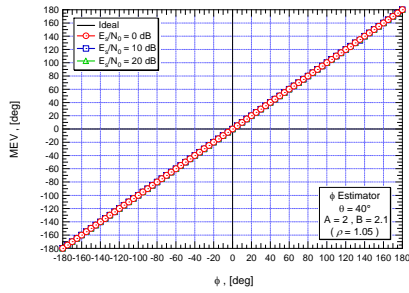


Fig. 3 – Simulated MEV of  $\phi$  for different values of  $E_s/N_0$ .

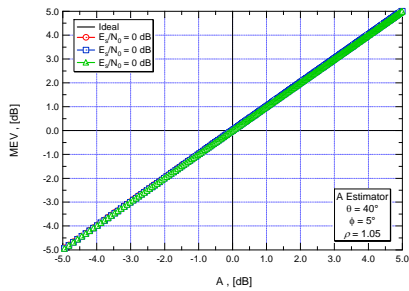


Fig. 4 – Simulated MEV of  $A$  for different values of  $E_s/N_0$ .

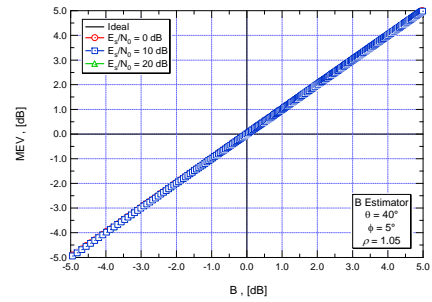


Fig. 5 – Simulated MEV of  $B$  for different values of  $E_s/N_0$ .

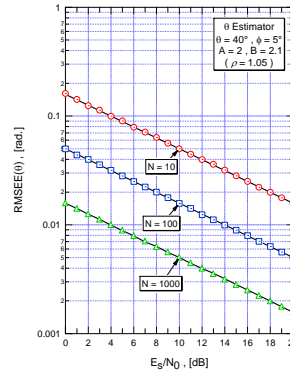


Fig. 6 – Simulated RMSEE of  $\theta$  (marks) and its CRB (solid lines) for different values of  $N$ .

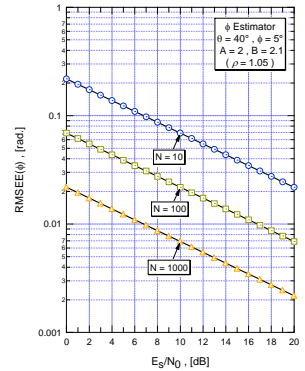


Fig. 7 – Simulated RMSEE of  $\phi$  (marks) and its CRB (solid lines) for different values of  $N$ .

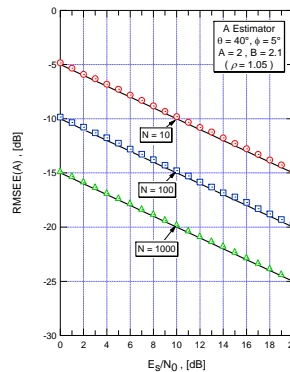


Fig. 8 – Simulated RMSEE of  $A$  estimator (marks) and its CRB (solid lines) for different  $N$ .

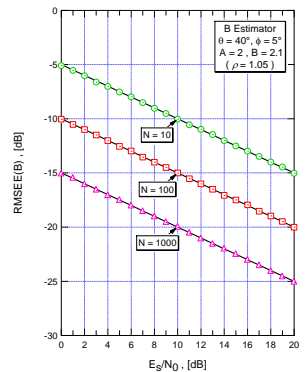


Fig. 9 – Simulated RMSEE of  $B$  estimator (marks) and its CRB (solid lines) for different  $N$ .

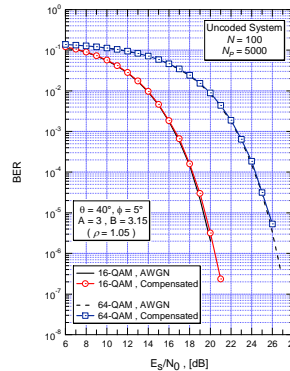


Fig. 10 – BER of uncoded 16-QAM and 64-QAM: AWGN and compensated receiver.

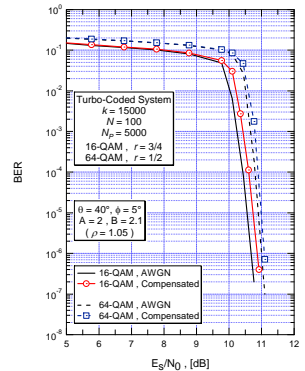


Fig. 11 – BER of turbo-coded 16-QAM and 64-QAM: AWGN and compensated receiver.